

# Supporting Information

## **Width-Consistent Mesoporous Silica Nanorods with a Precisely Controlled Aspect Ratio for Lysosome Dysfunctional Synergistic Chemo/Photothermal/Starvation/Oxidative Therapy**

Junna Lu<sup>a</sup>, Fengyu Liu<sup>b\*</sup>, Hongjuan Li<sup>a</sup>, Yongqian Xu<sup>a</sup>, Shiguo Sun<sup>a\*</sup>

<sup>a</sup>Shaanxi Key Laboratory of Natural Products & Chemical Biology, College of Chemistry & Pharmacy, Northwest A&F University, Xinong Road 22, Yangling, Shaanxi 712100, China

<sup>b</sup>State Key Laboratory of Fine Chemicals, School of Chemistry, Dalian University of Technology, No. 2 Linggong Road, Ganjingzi, District, Dalian 116023, China.

\*Corresponding authors:

Prof. Shiguo Sun (sunsg@nwsuaf.edu.cn)

Prof. Fengyu Liu (liufengyu@dlut.edu.cn)

# 1. EXPERIMENTAL SECTION

## 1.1 Materials.

Cetyltrimethylammonium bromide (CTAB), tetraethoxysilane (TEOS), aqueous ammonia ( $\text{NH}_3 \cdot \text{H}_2\text{O}$ ; 25-30 wt%), 3-aminopropyltriethoxysilane (APTES), fluorescein isothiocyanate (FITC), doxorubicin hydrochloride (DOX), Siramesine (Siram), dopamine hydrochloride (DA), trihydroxymethyl aminomethane (Tris), N-hydroxysuccinimide (NHS), 1-(3-dimethylaminopropyl)-3-ethylcarbodiimide (EDC), 3-[4,5-dimethylthiazol-2-yl]-2,5-diphenyltetrazolium bromide (MTT), dimethyl sulfoxide (DMSO), methanol, monopotassium phosphate ( $\text{KH}_2\text{PO}_4$ ), potassium chloride (KCl), sodium chloride (NaCl), disodium hydrogen phosphate ( $\text{Na}_2\text{HPO}_4$ ), Sodium hydroxide (NaOH) are analytical grade and obtained from Sigma-Aldrich (Shanghai, China). Bi-amino polyethylene glycol ( $\text{NH}_2\text{-PEG-NH}_2$ , Mw=2000) and folic acid (FA) were purchased from TCI (Shanghai, China). Hydrochloric acid (HCl), Hoechst 33342, 2,7-dichlorodihydrofluorescein diacetate (DCFH-DA) and Glucose oxidase (GOx) were purchased from Sigma Aldrich Corp. All chemicals were used as received without any further purification. All aqueous solutions were prepared with ultrapure Milli-Q water ( $\rho > 18.0 \text{ M}\Omega/\text{cm}$ ).

## 1.2 Measurement

UV-vis spectra were obtained on a Shimadzu 1750 UV-vis spectrometer. The size distribution and zeta potential of various nanoparticles were investigated by dynamic light scattering (DLS) with a ZEN3600 (MALVERN INSTRUMENTS LIMITED, UK). Thermogravimetric Analysis (TGA) was carried out on TGA/DSC 3+ (Switzerland).

The surface area, pore diameter and pore volume were tested on a Mike ASAP 2460 system. Cell toxicity tests were tested by microplate reader (KHB ST-360, Shanghai). A Quanta 200 environmental scanning electron microscope (SEM) (Nova Nano SEM-450) was used to observe the morphologies of the obtained materials. Transmission electron microscope (TEM) images were recorded with a TECNAI G2 SPIRIT BIO transmission electron microscope operating at 200 Kv. Fourier transform infrared (FT-IR) spectra were obtained on a MPA FT-IR spectrophotometer by a standard KBr disk method in the range 400-4000  $\text{cm}^{-1}$ . The nitrogen adsorption and desorption isotherms were measured at liquid  $\text{N}_2$  temperature using a MICROMERITICS ASAP 2460 instrument, after degassing samples for 12 h at 120 °C. Small angle x-ray diffraction (SAXRD, polycrystall X-ray diffraction, Rigaku Ultimate IV) was used to character the pore channel structure of nanoparticles. Raman spectra were obtained by using a dispersive spectrophotometer Jobin-Yvon LabRam HR Evolution with 532 nm light. Surface area was calculated according to the conventional Brunauer Emmett Teller (BET) method, and then the adsorption branches of the isotherms were used to calculate the pore parameters using the BJH method. The composition of the products was determined by X-ray photoelectron spectroscopy (XPS, Thermo ESCALAB 250XI). The image were acquired using a confocal fluorescence microscope (REVOLUTION WD).

### **1.3 Synthesis of NPs**

The synthesis of NPs with various ARs was based on published methods with a major modification.<sup>1</sup> In this study, a series of NPs were fabricated, the molar ratio of TEOS

and CTAB was keeping 7:1, which is a key factor for remaining the width of NPs unchanged. Under a constant  $\text{NH}_3 \cdot \text{H}_2\text{O}$  concentration and stirring rate, different AR of NPs can be acquired from 1 to 10, and finally to  $>10$ , with an increase concentration of CTAB and TEOS. Briefly, CTAB (3.24, 3.88, 4.53, 5.17, 6.47, 7.76, 9.06, 10.36 mM, respectively) was dissolved in 70 mL of  $\text{H}_2\text{O}$ , subsequently, 2 mL of  $\text{NH}_3 \cdot \text{H}_2\text{O}$  was added under a magnetic stirrer (220 rpm) for 1 h. Thereafter, TEOS was added in dropwise to the above solution and heated to 40 °C. After an additional 4 h of continuous stirring, the acquired white product was isolated by centrifugation (10000 rpm, 10 min) and washed several times with deionized water and ethanol. The surfactant template (CTAB) was removed by reflux condensation in a solution of 160 mL methanol solution containing 9 mL HCl (37%) refluxed at 80 °C for 12 h and washed with deionized water and ethanol for three times. The surfactant-free NPs was collected by centrifugation, and dried at 40 °C in a vacuum oven.

#### **1.4 Loading Drug into NPs**

100 mg of NPs were suspended in 20 mL of aqueous solution, and then 20 mL of the DOX·HCl (10 mg/mL) aqueous solution was added and stirred for 24 h and left overnight in the dark at room temperature. To remove the excess DOX, the solution was centrifuged and washed with deionized water three times. Subsequently, the DOX-loaded NPs were lyophilized and designated as NPs-DOX. All the washings were collected, and the drug loading capacity (LC) was evaluated from the difference between the concentration of initial DOX solution and that of the reaction medium combined with subsequent washings. DOX was determined by measuring the

absorption intensity at wavelength of 480 nm by a UV-vis spectrometer. The load experiments were conducted in six times. The drug LC was calculated using the following equation:<sup>2</sup>

$$\text{Drug LC (\%)} = \frac{\text{weight of drug in the NPs}}{\text{weight of drug in the NPs} + \text{weight of NPs}} \times 100\%$$

### **1.5 In Vitro DOX Release Profile**

To compare the release profile of DOX from NPs-DOX, NPs-DOX (2 mg) was incubated in 1 mL of PBS (pH 7.4, 10 mM), and then transferred into a dialysis bag (MW=3500 Da) and put into 20 mL of PBS with gentle stirring (100 rpm). At appropriate time intervals, 2 mL of the external release medium from each group was collected for concentration determination and replaced with an equal volume of fresh medium. DOX was determined by measuring the absorption intensity at wavelength of 480 nm by a UV-vis spectrometer.

### **1.6 Synthesis of NPs-FITC**

The surfaces of NPs were functionalized by the addition of primary amines, using APTES to attach alkoxy silane groups to surface hydroxides. To compare the cellular uptake efficiency, it is necessary to regulate the amount of FITC to ensure the NPs labeled with equal amounts of FITC. At first, The FITC-modified APTES (FITC-APTES) was obtained, 400  $\mu$ L of APTES was added to 1 mL of absolute ethanol with different FITC concentrations over a range of 13.7 to 25 mM. The reaction mixture was magnetic stirring for 2 h in the dark. Subsequently, FITC-APTES was added to 50 mL NPs solution (2 mg/mL in absolute ethanol) under magnetic stirring and heated to 80 °C. After another 6 h, the precipitant was collected by washing with deionized water and

absolute ethanol. Finally, the NPs-FITC were dried with a vacuum oven at 80 °C overnight.

## **1.7 Cell Culture**

In a humidified 5% CO<sub>2</sub> atmosphere, HL7702 (human normal liver cells) and HepG2 (human liver carcinoma cell line) cells were cultured at 37 °C in RPMI 1640 medium supplemented with 10 v/v% fetal bovine serum (FBS) and 1 v/v% antibiotics (complete 1640). For cell passage, 0.25% trypsin solution was used for digesting cells.

## **1.8 Cell Imaging**

To compare the cellular uptake efficiency, HepG2 and HL7702 cells were used for cell imaging. Cells were seeded in 35 mm plastic-bottomed  $\mu$ -dishes for 24 h. Then, the culture medium was discarded and replaced by a fresh medium containing with NPs-FITC at 60  $\mu$ g/mL. After incubation 0.5, 1, 2, 4 h, the medium was removed and the cells were washed twice with PBS. Subsequently, the cells were stained with Hoechst 33342, after 15 min of incubation, the cells were rinsed softly by PBS to perform fluorescence imaging with a CLSM. Blue and green luminescent emissions from Hoechst 33342 and FITC were excited at the wavelength of 346 nm and 488 nm, respectively. The emission wavelengths were ranged from 460 nm to 475 nm for Hoechst 33342 and 500 nm to 550 nm for FITC. There was no interference between these two channels. The scanning mode was in sequential frame.

## **1.9 Quantification of NPs-FITC Uptake**

To quantify the cellular uptake efficiency, HepG2 and HL7702 cells were seeded in six-well culture plates and grown overnight. Then, the culture medium was discarded

and replaced by a fresh medium containing with NPs-FITC at 60  $\mu\text{g/mL}$  for 0.5, 1, 2, and 4 h. A single cell suspension was prepared consecutively by trypsin, collected through centrifugation at 1200 rpm for 5 min and washing with PBS for three times, and filtration through a nylon mesh filter (300 mesh). Finally, the cells were quickly analyzed using a flow cytometer (BD FACS Aria<sup>TM</sup> III, USA) for FITC. Data were analyzed with Flowjo software.

### **1.10 Cell Viability**

The cytotoxicity of NPs against HL7702 and HepG2 cells at different concentrations was evaluated by typical MTT assay. HL7702 and HepG2 cells were seeded in 96-well plate at a density of  $1 \times 10^4$  cells per well and cultured for 24 h, and then different concentrations of NPs were added. After 24 h of incubation, the fresh medium containing MTT (0.5 mg/mL) was added into each well. After another 4 h of incubation, the medium containing MTT was removed and DMSO (100  $\mu\text{L}$ ) was added to each well to dissolve the formazan crystals. Finally, the plate was gently shaken for 10 min and the absorbance at 490 nm was recorded with a microplate reader.

### **1.11 Preparation of Amino-Functionalized AR6**

We synthesized AR6-NH<sub>2</sub> according to a reported work with slight modifications.<sup>3</sup> The surface of AR6 was functionalized with amine groups by treatment with APTES. First, AR6 (50 mg) was dispersed in 100 mL of ethanol and heated to 80 °C for 4 h. Then, 100  $\mu\text{L}$  of APTES was added to the above solutions and refluxed for another 6 h. After centrifugation and washing with water, amine-functionalized AR6 designed as AR6-NH<sub>2</sub> was acquired.

### **1.12 Synthesis of GOx-FITC**

In order to investigate the cellular uptake of nanosystem, we synthesized GOx-FITC according to the previous study with slight modifications.<sup>4</sup> Briefly, GOx (8 mg) was dissolved in 3 mL of sodium bicarbonate solution (100 mM). Then, 1 mL of prepared FITC solution (4 mg/mL in DMSO) was added in dropwise under magnetic stirring and the mixture was stirred at room temperature for 4 h in the dark. The resulting FITC labeled GOx (designed as GOx-FITC) was further dialyzed in PBS solution for 3 days to remove unreacted residues. GOx-FITC was frozen at -80 °C and lyophilized overnight.

### **1.13 DOX and GOx Loading**

100 mg of AR6-NH<sub>2</sub> were suspended in 20 mL of aqueous solution, and 20 mL of the DOX·HCl (10 mg/mL) aqueous solution was added and stirred for 24 h and left overnight in the dark at room temperature. The loaded AR6-NH<sub>2</sub> (designed as AR6-DOX) was collected by centrifugation (12000 rpm, 15 min). Subsequently, 20 mL of GOx aqueous solution (1 mg/mL) was mixed with 20 mL of AR6-DOX (10 mg/mL) and incubated at 4 °C overnight (designed as AR6-DOX-GOx).

### **1.14 PDA Surface Modification**

40 mg of AR6-DOX-GOx was dispersed in 10 mL of Tris-HCl buffer (pH 8.5, 10 mM). DA (40 mg) was dissolved in 10 mL of Tris-HCl buffer and then added into the AR6-DOX-GOx solution under magnetic stirring and mixture was stirred at room temperature in the dark. After 10 h of stirring, the obtained black products were centrifuged and rinsed several times with deionized water to remove the unpolymerized



dopamine and then dried by lyophilization. The surface-modified products were designated as AR6-DOX-GOx@PDA. Blank sample (drug-free AR6) was also prepared by the same method and denoted as AR6@PDA.

### **1.15 Conjugation of PEG-FA to AR6-DOX-GOx@PDA**

The functional ligands were bound to the surface of the AR6-DOX-GOx@PDA via Michael addition reaction.<sup>5</sup> Briefly, 30 mg of AR6-DOX-GOx@PDA was resuspended in 30 mL of Tris-HCl buffer containing 30 mg of the NH<sub>2</sub>-PEG-NH<sub>2</sub> and was stirred for 12 h at room temperature. The obtained product was centrifuged and washed with deionized water to remove residual reactants. The conjugation of FA onto AR6-DOX-GOx@PDA-PEG was obtained through an amide reaction. 30 mg of EDC, 30 mg of NHS, 5 mL of FA (6 mg/mL in DMSO) were mixed in 30 mL of PBS under magnetic stirring for 2 h at 4 °C in the dark. Then, 3 mL of AR6-DOX-GOx@PDA-PEG (10 mg/mL) solution was added in dropwise to the above solution. After 24 h of stirring at room temperature, the resulting products were collected and further removed residual reactants. The final product was lyophilized, for convenience, AR6-DOX-GOx@PDA-PEG-FA was abbreviated as AR6-DOX-GOx@PDA-FA. Blank sample (drug-free AR6) was also prepared and denoted as AR6@PDA-FA.

### **1.16 Siram Loading onto The Exterior Surface**

The solutions of AR6-DOX-GOx@PDA-FA (1 mg/mL in Tris-HCl buffer) was mixed with different concentration of Siram (1, 2, 3, 4 mg/mL) in Tris-HCl buffer. After 24 h of stirring at room temperature in the dark, excess Siram was removed with Tris-HCl buffer by centrifugation and the concentration was calculated by calibration

curve of Siram. The final product was denoted as AR6-DOX-GOx@PDA-FA-Siram.

### **1.17 Photothermal Properties**

To evaluate the photothermal effect, water, AR6, AR6@PDA and AR6@PDA-FA were determined the temperature changes at 200  $\mu\text{g/mL}$  under 808 nm NIR irradiation at 1.0  $\text{W/cm}^2$  for 600 s. Subsequently, various concentrations of AR6@PDA-FA solutions (50, 200, and 400  $\mu\text{g/mL}$ , respectively) were done under 808 nm NIR irradiation at 1.0  $\text{W/cm}^2$  for 600 s. To investigate the influence of power density on the photothermal effect, AR@PDA-FA solution (200  $\mu\text{g/mL}$ ) was exposed to different power densities of 0.5, 1, 1.5, 2  $\text{W/cm}^2$  for 600 s, respectively. The photothermal stability of AR@PDA-FA solution (200  $\mu\text{g/mL}$ ) was characterized by on/off irradiation for recording the temperature change curves and the repeated heating-cooling cycles. Briefly, the suspension was first irradiated for 600 s, followed by naturally cooling for 600 s and this was alternately repeated for 5 cycles.

In detail, 3 mL aqueous dispersions of samples were exposed to a continuous-wave diode NIR irradiation for 600 s over a range of concentrations in quartz cuvette. The laser spot was focused on the center of the sample. The solution temperature was dynamically recorded using a digital thermometer (precision: 0.1  $^{\circ}\text{C}$ ) with a thermocouple probe at intervals of 10 s during NIR irradiation.

### **1.18 In Vitro Drug Release Profile**

In vitro DOX and Siram release profile of AR6-DOX-GOx@PDA-FA-Siram was detected by the dialysis method. 1 mL of AR6-DOX-GOx@PDA-FA-Siram solution (5  $\text{mg/mL}$  in PBS) was encapsulated into a dialysis bag (MWCO=3500 Da) and put

into 20 mL of PBS at different pH (7.4 or 5.0) shaken at 37 °C and 120 rpm. In order to assess PDA degradation under NIR irradiation can accelerate drug release, the above samples were vertically irradiated (1 W/cm<sup>2</sup>) for 10 min at prescribed times (2, 4, 8, 12 h). In addition, AR6-DOX-GOx was conducted to confirm the gatekeeper of external PDA at pH 7.4. At appropriate time intervals, 2 mL of the outside release solution was taken out and replenished with fresh buffer of equal volume and the whole released DOX and Siram was measured using UV-vis spectrometer. In the assessment of drug release behavior, the cumulative amount of released drug was calculated, and the relationship between accumulative release from nanosystem was plotted against time. All release experiments were carried out in five times.

### **1.19 Visualization of Codelivery of DOX and GOx-FITC**

The detailed procedure was indicated in section 1.8 above, briefly, AR6-DOX-GOx@PDA-FA (0.1 µg/mL of GOx, DOX of 1 µg/mL) was incubated with HepG2 cells for 1, 2, 3, 4 h, respectively. Subsequently, DOX+GOx, AR6-DOX-GOx@PDA, AR6-DOX-GOx@PDA-FA and AR6-DOX-GOx@PDA-FA+FA were incubated with HepG2 and HL7702 cells for 4 h. For FA-preincubation groups, HepG2 and HL7702 cells were first incubated with FA (100 µM) for 30 min. Subsequently, the cells were stained with Hoechst 33342.

### **1.20 Intracellular reactive oxygen species (ROS) Assay**

To monitor the intracellular ROS levels in HepG2 cells, CLSM and FACS were carried out, the detailed procedure was indicated in the above section 1.8 and 1.9. HepG2 cells were incubated for 6 h with (1) PBS, (2) AR6@PDA, (3) DOX, (4) GOx,

(5) Siram, (6) AR6-DOX-GOx, (7) AR6-DOX-GOx@PDA, (8) AR6-DOX-GOx@PDA-FA, (9) AR6-DOX-GOx@PDA-FA-Siram, and (10) AR6-DOX-GOx@PDA-FA-Siram+FA, at concentrations of DOX, GOx, and Siram of 1  $\mu\text{g/mL}$ , 0.1  $\mu\text{g/mL}$  and 2  $\mu\text{M}$ . In addition, to explore the introduction of PDA (photothermal material) can rise temperature and accordingly elevating the catalytic efficiency of GOx. The groups were irradiated with an NIR irradiation (808 nm, 1.0 W/cm<sup>2</sup>, 10 min). Subsequently, the cells were washed with PBS for three times and the media was replaced with DCFH-DA (10  $\mu\text{M}$ ) for 20 min. DCF decomposed from DCFH-DA was excited at 488 nm, and fluorescence was detected from 500 to 550 nm.

### **1.21 Lysosome Dysfunction**

To investigate the lysosomal activity, CLSM and FACS were carried out, the detailed procedure was indicated in the above section 1.8 and 1.9. HepG2 cells were incubated for 6 h with (1) PBS, (2) AR6-DOX-GOx@PDA-FA, (3) AR6-DOX-GOx@PDA-FA+NIR, (4) Siram, (5) AR6-DOX-GOx@PDA-FA-Siram, (6) AR6-DOX-GOx@PDA-FA-Siram+NIR. Afterward, the cells were stained with LysoTracker Green (100 nM) for 20 min. The excitation and emission wavelengths for determination were 504 and 511 nm, respectively.

### **1.22 In Vitro Synergic Therapeutic Efficacy and Cytotoxicity Assay**

The cell viabilities were evaluated by MTT assay, the detailed procedure was as indicated in the above section 1.10. HepG2 and HL7702 cells were incubated for 24 h with (1) DOX, (2) GOx, (3) DOX+GOx, (4) AR6-DOX-GOx, (5) AR6-DOX-GOx@PDA, (6) AR6-DOX-GOx@PDA-FA, (7) AR6-DOX-GOx@PDA-FA+FA, and

(8) AR6-DOX-GOx@PDA-FA-Siram at different concentrations. To evaluate synergic therapeutic efficiency, after 4 h of incubation, the cells were irradiated with an NIR irradiation (808 nm, 1.0 W/cm<sup>2</sup>, 10 min), and then incubated for another 20 h.

To ensure the safety of biological applications, HepG2 and HL7702 cells were incubated for 24 h with AR6, AR6@PDA and AR6@PDA-FA at different concentrations (1, 10, 50, 100, 250 µg/mL). Subsequently, to study photothermal cytotoxicity of PDA shell, cells were incubated with AR6, AR6@PDA and AR6@PDA-FA at different concentrations (5, 10, 20, 40, 60 µg/mL). After 4 h of incubation, the cells were irradiated under an NIR irradiation (808 nm, 1.0 W/cm<sup>2</sup>, 10 min), and then incubated for another 20 h. As a control, blank cells were also tested under the same conditions.

### **.1.23 Statistic Analysis**

The significance of the data was assessed according to two-way analysis of variance (ANOVA): \* $p < 0.05$ , \*\* $p < 0.01$ , \*\*\* $p < 0.001$  and \*\*\*\* $p < 0.0001$ . The samples were distributed to experimental groups and processed randomly. The data analysis was analyzed using GraphPad Prism (Version 7.0, GraphPad Software, Inc., San Diego, USA).

## 2. SUPPLEMENTARY FIGURES

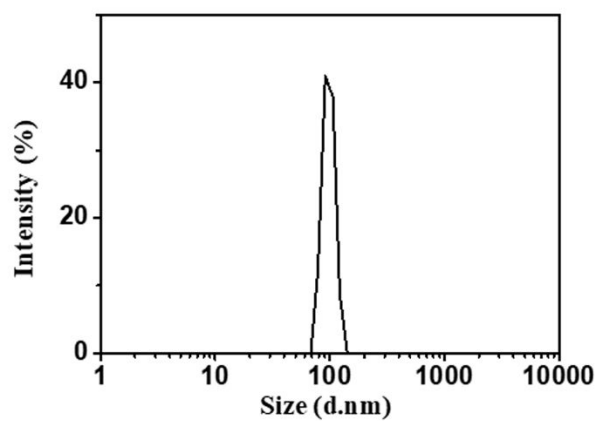


Fig. S1. Size distribution of MSN.

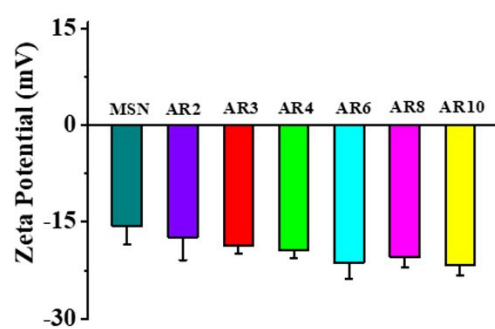


Fig. S2. Zeta potentials of different NPs. All data points represented as mean  $\pm$  s.d. ( $n = 5$ ).

Table S1. Related Parameters of different NPs.

NPs	AR (length/width)	Length (nm)	Width (nm)	Zeta Potential (mV)	Surface Area (m <sup>2</sup> /g)	Pore Volume (cm <sup>3</sup> /g)	Pore Size (nm)
MSN	1	102.13±10.23	103.03±9.65	-15.71	874.42	0.83	3.81
AR2	2	201.32±8.21	98.96±5.26	-17.43	699.15	0.50	2.85
AR3	3	299.25±15.56	97.62±3.26	-18.66	769.75	0.62	3.21
AR4	4	403.42±18.63	102.24±6.48	-19.41	773.11	0.85	4.39
AR6	6	600.58±20.34	100.88±7.56	-21.32	1021.77	0.86	3.36
AR8	8	807.25±19.05	101.61±7.55	-20.44	977.34	0.85	3.48
AR10	10	1004.72±52.32	101.25±6.38	-21.63	1224.23	1.22	3.41

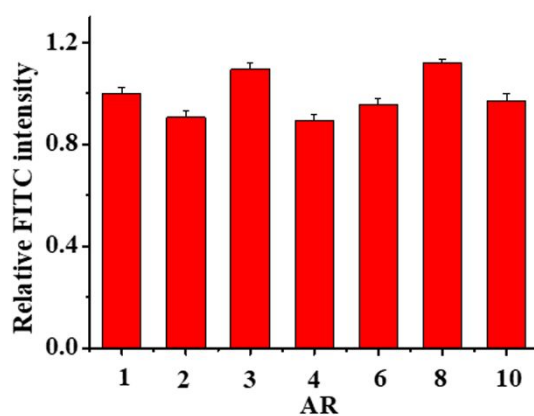


Fig. S3. FITC labeling efficiency of the different NPs. All data points represented as mean ± s.d. (n = 5).

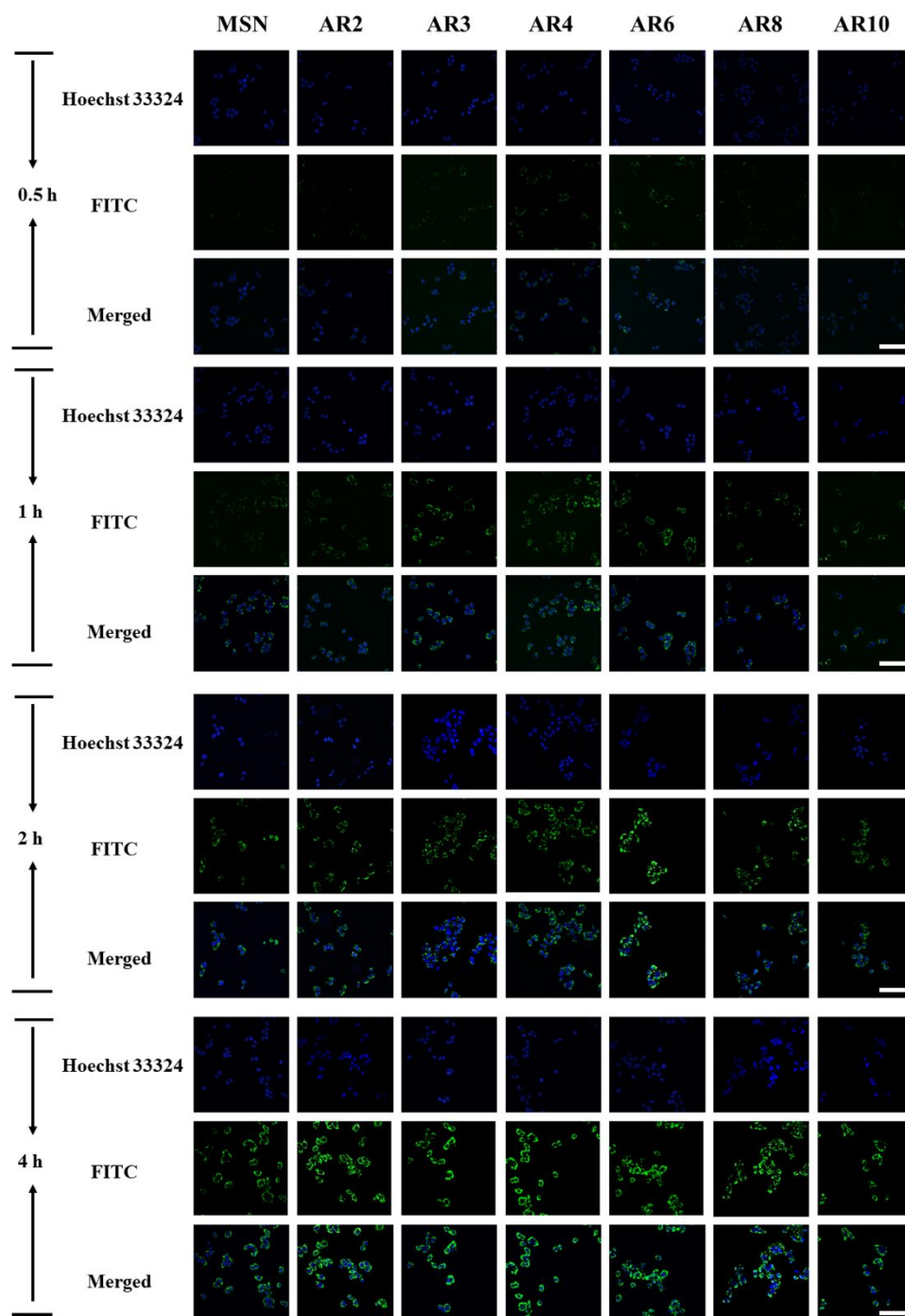


Fig. S4. The CLSM images of HL7702 cells incubated 0.5, 1, 2, 4 h with different NPs-FITC at 60  $\mu\text{g/mL}$ , respectively. Blue and green fluorescence were revealed via Hoechst 33324 and FITC, Scale bars: 100  $\mu\text{m}$ .



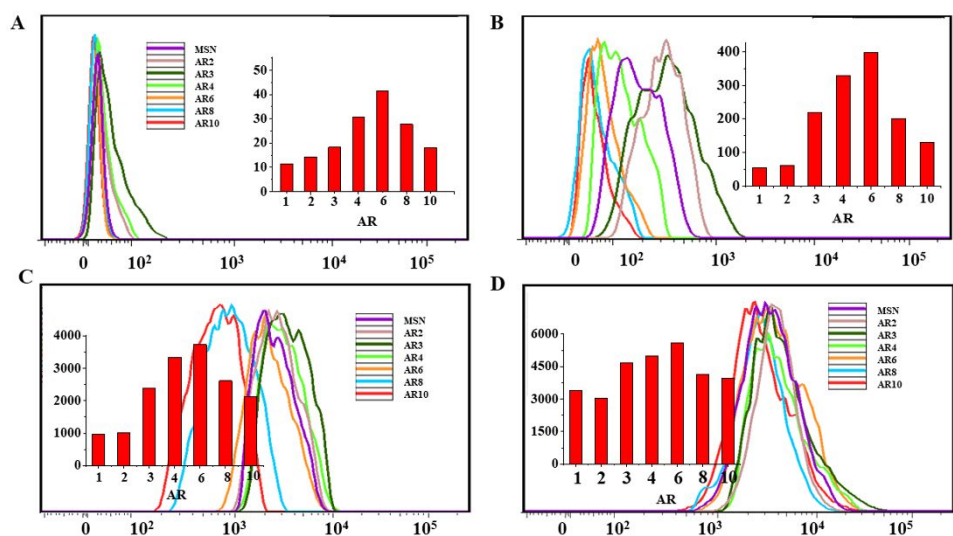


Fig. S5. Flow cytometric profiles of HL7702 cells incubated A) 0.5 h; B) 1 h; C) 2 h; D) 4 h with different NPs-FITC at 60 µg/mL, respectively. Inset: Quantitative analysis of MFI.

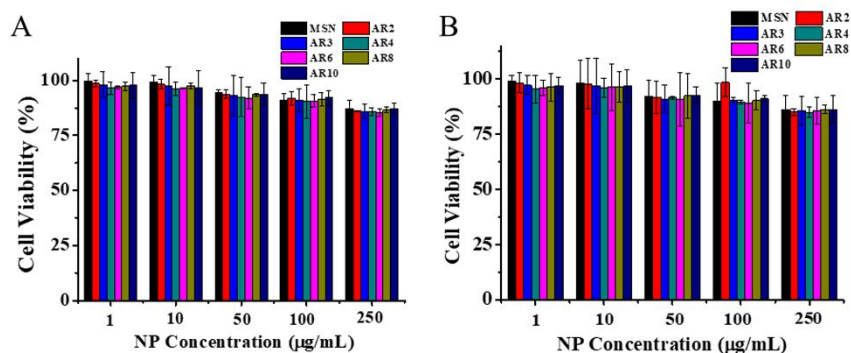


Fig. S6. Relative viabilities of A) HepG2 and B) HL7702 cells after various samples of treatment at different concentrations for 24 h. All data points represented as mean  $\pm$  s.d. (n = 5).

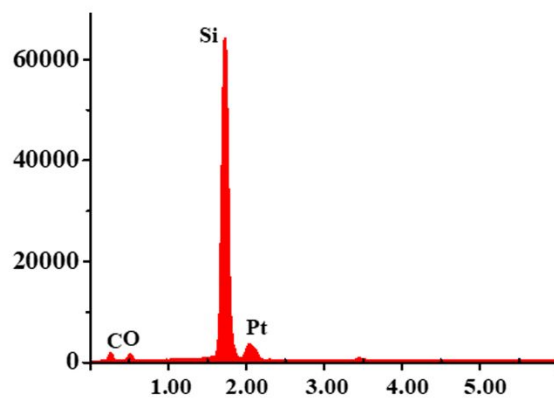


Fig. S7. EDS spectrum of AR6.

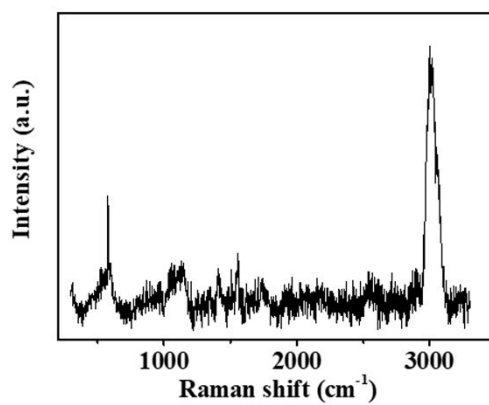


Fig. S8. Raman spectra of AR6- $\text{NH}_2$ .

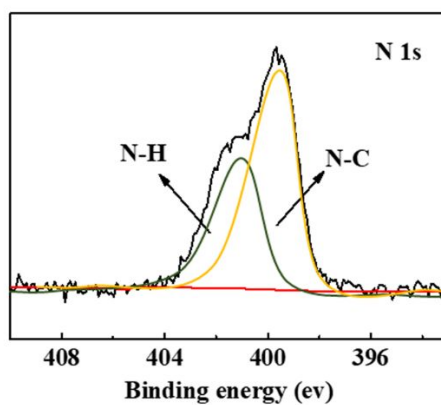


Fig. S9. N 1s XPS spectra of AR6- $\text{NH}_2$ .

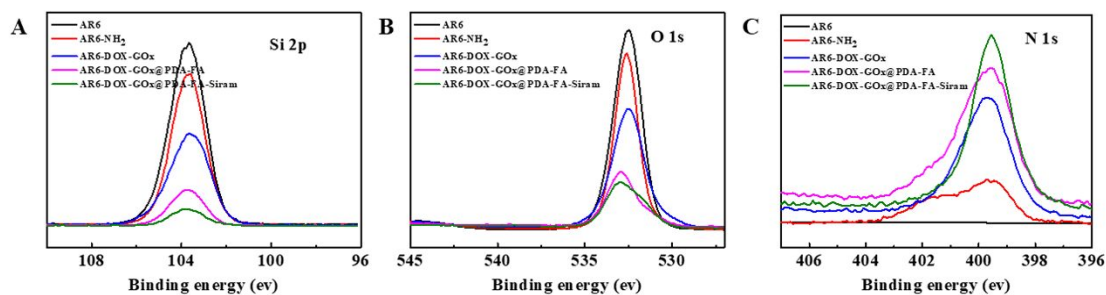


Fig. S10. XPS spectra of A) Si 2p spectrum, B) O 1s spectrum and C) N 1s spectrum.

Table S2. Related Parameters of Different samples.

	Surface Area (m <sup>2</sup> /g)	Pore Volume (cm <sup>3</sup> /g)	Pore Size (nm)
AR6	1021.77	0.86	3.36
AR6-DOX	490.10	0.16	1.39
AR6-DOX-GOx	414.77	0.14	1.27
AR6-DOX-GOx@PDA-FA	229.97	0.08	N/A
AR6-DOX-GOx@PDA-FA-Siram	178.43	0.06	N/A

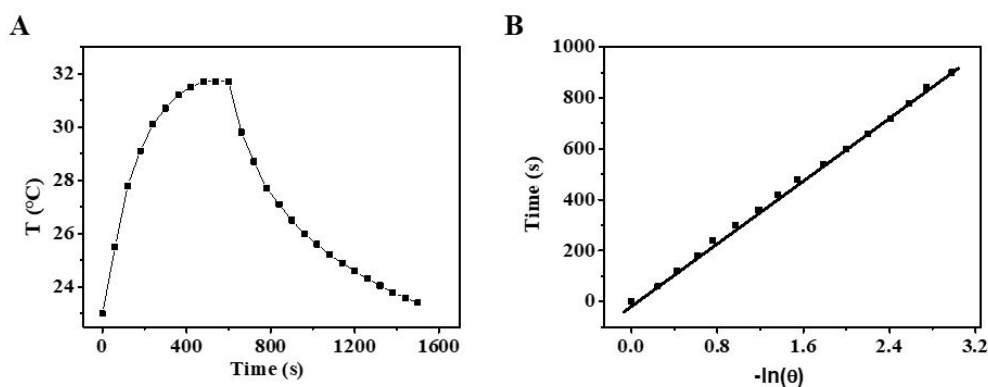


Fig. S11. A) Photothermal effects of AR6@PDA-FA (200  $\mu\text{g/mL}$ ) under NIR irradiation (1.0 W/cm<sup>2</sup>) for 600 s and then stopping the irradiation. B) Linear fitting of time data versus  $-\ln \theta$  obtained from the cooling period of AR6@PDA-FA.

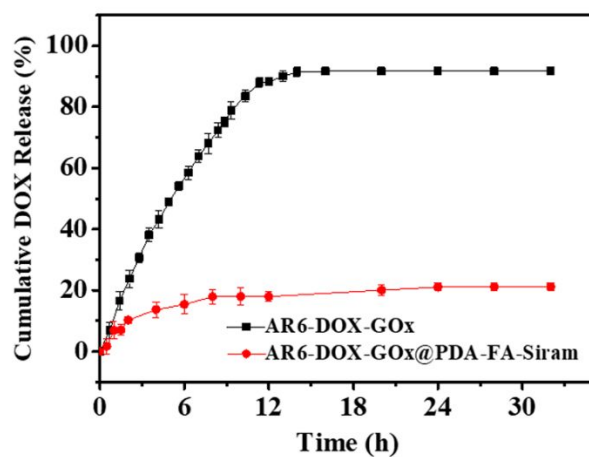


Fig. S12 The DOX release profiles of AR6-DOX-GOx and AR6-DOX-GOx@PDA-FA-Siram at pH 7.4, 37 °C. All data points represent as mean  $\pm$  s.d. (n = 5).

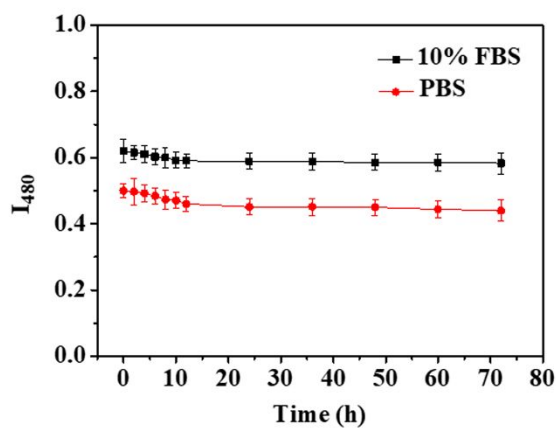


Fig. S13 Stability of AR6-DOX-GOx@PDA-FA-Siram at PBS (pH 7.4) and 10% FBS. All data points represent as mean  $\pm$  s.d. (n = 5).

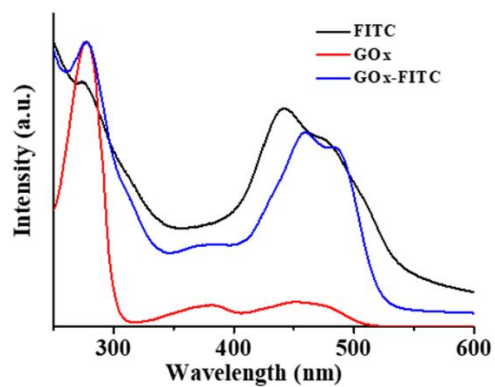


Fig. S14. Absorption spectra of FITC, GOx and GOx-FITC.

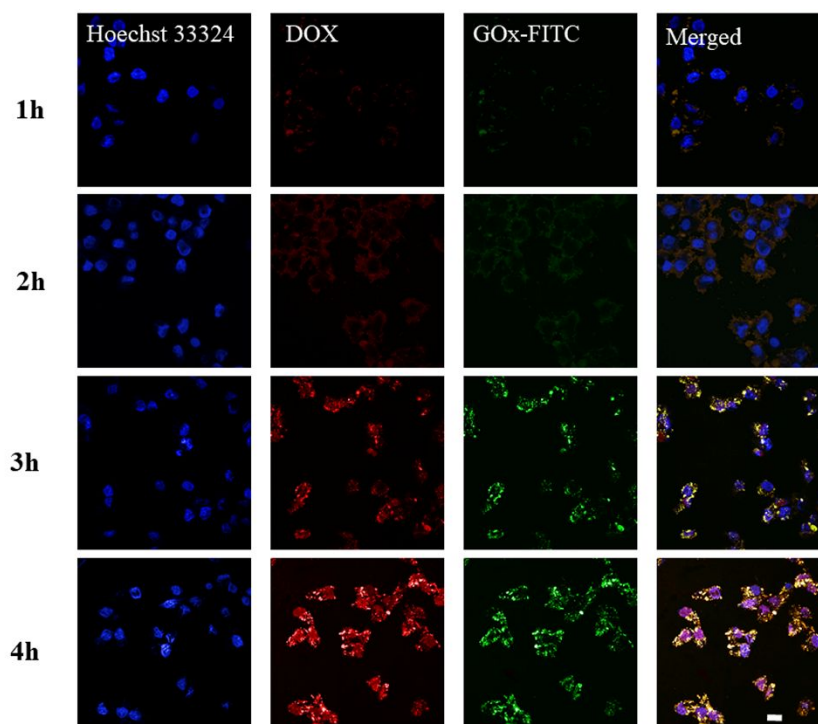


Fig. S15. CLSM images of HepG2 cells incubated 1, 2, 3, 4 h with AR6-DOX-GOx@PDA-FA.

Blue, green and red fluorescence were revealed via Hoechst 33324, FITC and DOX, Scale bar: 20  $\mu\text{m}$ .

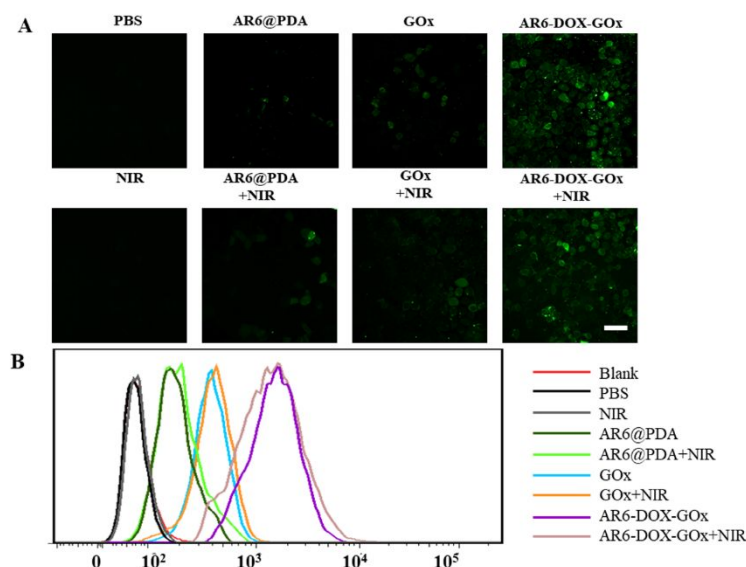


Fig. S16. A) CLSM images and B) Flow cytometric profiles of HepG2 cells incubated 6 h with various samples in the absence or presence of  $1.0 \text{ W/cm}^2$  NIR irradiation for 10 min and then stained with DCFH-DA. Scale bars:  $50 \mu\text{m}$ .

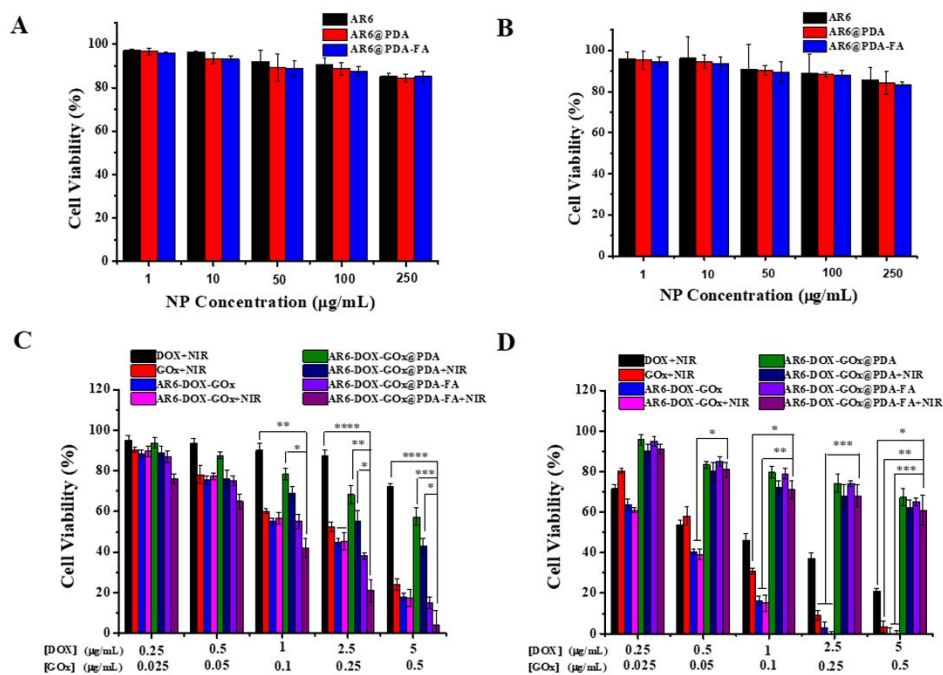


Fig. S17. Relative viabilities of A, C) HepG2 and B, D) HL7702 cells after various samples of treatment at different concentrations for 24 h and in the absence or presence of  $1.0 \text{ W/cm}^2$  NIR irradiation for 10 min. All data points represent as mean  $\pm$  s.d. ( $n = 5$ ) (\* $p < 0.05$ , \*\* $p < 0.01$ , \*\*\* $p < 0.001$  and \*\*\*\* $p < 0.0001$ ).

## REFERENCES

- (1) Huang, X.; Teng, X.; Chen, D.; Tang, F.; He, J., The effect of the shape of mesoporous silica nanoparticles on cellular uptake and cell function. *Biomaterials* **2010**, *31* (3), 438-448.
- (2) Yang, N.; Ding, Y.; Zhang, Y.; Wang, B.; Zhao, X, Surface Functionalization of Polymeric Nanoparticles with Umbilical Cord-Derived Mesenchymal Stem Cell Membrane for Tumor-Targeted Therapy. *ACS Appl. Mater. Interfaces* **2018**, *10*, 22963–22973.
- (3) Pan, L.; Liu, J.; He, Q.; Shi, J., MSN-mediated sequential vascular-to-cell nuclear-targeted drug delivery for efficient tumor regression. *Adv. Mater.* **2014**, *26* (39), 6742-6748.
- (4) Li, J.; Li, Y.; Wang, Y.; Ke, W.; Chen, W.; Wang, W.; Ge, Z., Polymer prodrug-based nanoreactors activated by tumor acidity for orchestrated oxidation/chemotherapy. *Nano Lett.* **2017**, *17* (11), 6983-6990.
- (5) Lu, W.; Liao, Y.; Jiang, C.; Wang, R.; Shan, X.; Chen, Q.; Sun, G.; Liu, J., Polydopamine-coated NaGdF<sub>4</sub>: Dy for T<sub>1</sub>/T<sub>2</sub>-weighted MRI/CT multimodal imaging-guided photothermal therapy. *New J. Chem.* **2019**, *43* (19), 7371-7378.